Weather and Climate Extremes 25 (2019) 100218

Contents lists available at ScienceDirect

Weather and Climate Extremes

journal homepage: www.elsevier.com/locate/wace

Winter pressures on the UK health system dominated by the Greenland Blocking weather regime

Andrew J. Charlton-Perez[a,*], Robert W. Aldridge[b], Christian M. Grams[c], Robert Lee[a,d]

[a] Department of Meteorology, Univ. of Reading, Reading, UK
[b] Farr Institue, University College London, London, UK
[c] Institute for Meteorology and Climate Research (IMK-TRO), Karlsruhe Institute of Technology (KIT), Karlsruhe, Germany
[d] National Centre for Atmospheric Science, University of Reading, Reading, UK

ARTICLE INFO

Keywords:
Mortality
Health system
Cold weather
Weather regimes

ABSTRACT

In many countries, wintertime cold weather is linked to ill-health and intense pressure on public health services. This study examines how both long-term climate change and sub-seasonal variability contribute to the temperature extremes that increase pressures on the UK's National Health Service. The impact of temperature on fractional mortality and hospital admissions due to chronic obstructive pulmonary disease are used as metrics of wintertime pressure on the health system. The focus of the study is on days during the year in which the fractional mortality and hospital admissions attributable to cold weather exceed the five-year return period. These days are henceforth called winter pressure days since they likely to lead to significant pressure on the health service to meet demand. On interdecadal and longer timescales, winter pressure days show a robust decline over recent decades with a reduction from a probability of 0.29 in the pre-industrial period to 0.11 for the period 2000–2016. Comparing the risk of winter pressure days in two different climate model simulations of the historical period and a counterfactual ensemble of only natural climate forcings shows that this decline can be clearly attributed to anthropogenic activity. The average Fraction of Attributable risk due to anthropogenic activity for these two climate models for winter pressure days is −0.94. On sub-seasonal timescales, weather drivers of winter pressure days are assessed through analysis of diagnostics of weather regime lifecycles. This analysis shows winter pressure days occur almost exclusively in the Greenland Blocking regime. Although the risk of winter pressure days is likely to continue to decline with current climate trends, there remains a substantial weather driven risk to the UK health system. Preparing for weather events that cause stress on the system should focus on the analysis and prediction of the Greenland Blocking regime on weekly timescales.

1. Introduction and motivation

Cold weather in the UK and in other countries is associated with increases in mortality from a range of primarily cardiovascular and respiratory conditions, as reviewed comprehensively in Hajat (2017). Typically, epidemiological studies for the UK (e.g. Hajat et al., 2007) show a U or V-shaped relationship between temperature and the number of deaths (henceforth, mortality) with increases in mortality when temperatures drop below a moderate threshold of 5–6°C. Cold weather impacts on mortality typically peak 2–3 days after the occurrence of cold temperatures and can persist for up to 20 days (Gasparrini et al., 2015). Additional mortality associated with cold weather is not the result of a displacement of deaths that would have occurred subsequently (Analitis et al., 2008). Enhanced mortality associated with moderate and severe cold is common in cities outside of the tropics (Gasparrini et al., 2015), although understanding of differences in vulnerability to exposure to cold conditions in different climate regimes is still limited (Liddell et al., 2016).

The National Health Service (NHS) in the UK is under increasing pressure to provide high-quality healthcare to the UK population (Iacobucci, 2017). Winter capacity issues in the NHS are driven by a wide range of factors in addition to temperature, including increasing numbers of patients with long-term medical conditions (Hull et al., 2018), delays in the transfer of patients between different parts of the service (Gardner, 2018) and the prevalence of communicable diseases which peak during the winter such as influenza (Hawkes, 2018). Pressures on the hospital system are most acute during winter, as hospital admissions peak, partly in response to increases in respiratory disease linked to cold weather (Elliot et al., 2008). During winter 2017/18, the NHS cancelled many appointments to deal with extreme

* Corresponding author.
E-mail address: a.j.charlton-perez@reading.ac.uk (A.J. Charlton-Perez).

https://doi.org/10.1016/j.wace.2019.100218
Received 16 January 2019; Received in revised form 4 June 2019; Accepted 25 July 2019
Available online 30 July 2019

demands on the service during cold periods in early-January and early-March (Iacobucci, 2018). Planning for the future of health service provision requires understanding of different meteorological drivers modulate winter pressures on the NHS during this and other years. Long-term projections of the impacts of the changing climate on total cold related mortality Hajat et al. (2014) suggest only small changes by 2050, despite long-term anthropogenically driven increases in temperature and a concomitant decrease in cold conditions in the UK. This is partly due to the growing and ageing population of the UK that increases the vulnerability to cold weather conditions, offsetting any reduction in mortality due to the warming climate. To-date, however, there has been little study of if and how cold-related health impacts have changed over the recent past.

As climate warms, cold temperatures in the UK and Northern Europe are expected to become less common. de Vries et al. (2012) show that, for example, that minimum temperatures associated with the most extreme cold periods are projected to increase by 5°C by the end of the 21st century in climate model runs forced with the SRES A1b scenario. A number of attribution studies have shown clearly that the risk of very cold winters, similar to those observed in 2009/10 and 2010/11, has already significantly declined (Peterson et al., 2012; Christidis et al., 2013). These results suggest that the probability of a winter like 2009/10 has declined by eight times compared to what might have been experienced in a world without anthropogenic climate forcings and that the probability of winter like 2010/11 has halved.

This study has two main scientific objectives. Firstly, we seek to quantify if the observed decrease in the likelihood of cold winters has driven a reduction in the risk of extremes of cold-weather health impacts in the UK. A similar end-to-end attribution approach (Stone and Allen, 2005) has been demonstrated for heat-related deaths during the summer of 2003 by (Mitchell et al., 2016), who demonstrated that anthropogenic climate change had increased the likelihood of extreme heat related mortality by 70% in central Paris and 20% in London. Our focus is on daily extremes of mortality and hospital admissions due to the exacerbation of Chronic Obstructive Pulmonary Disease (COPD). These metrics are used to provide information about periods of extreme stress on the health system in the UK. We assume that extremes of mortality and hospital admissions are also periods in which the capacity of health system is placed under pressure over winter. Henceforth, we refer to these extremes as *winter pressure days* so that it is clear that our interest here is on periods during the year in which the health system is placed under acute stress.

Secondly, we aim to understand the main meteorological drivers of winter pressure days in the UK. Our focus is on the large-scale atmospheric flow conditions and so our focus will be on European Weather Regimes (WRs). WRs are often used to characterise large-scale atmospheric conditions. Weather regimes are quasi-stationary, persistent, and recurrent atmospheric flow patterns, that determine the character of weather for several days to a few weeks and affect continent-size regions (e.g. Vautard (1990); Michelangeli et al. (1995); Ferranti et al. (2015)). There are four typical, prevailing weather regimes in the North-Atlantic European region in winter: The "Zonal Regime" (ZO) dominated by low pressure in the Icelandic region, "Greenland Blocking" (GL) with a blocking high pressure systems near southern Greenland, "Atlantic Ridge" (AR) with a blocking ridge in the central North Atlantic, and the "Blocking Regime" (BL) with a blocking high pressure system in the North Sea region (Yiou and Nogaj, 2004; Neal et al., 2016; Hall and Hanna, 2018). The Zonal and Greenland Blocking regimes correspond to the positive and negative phases of the North-Atlantic Oscillation (NAO), respectively. In contrast to the NAO, weather regimes describe the full-range of multi-day variability of weather in the European region.

By comparing both long-term climate and short-term meteorological drivers of winter pressure days using the same underlying framework, it is possible to understand the extent to which long-term planning (e.g. Public Health England, 2017) needs to account for each component of climate system variability.

2. Datasets and methodology

2.1. Datasets

2.1.1. Temperature data

The Central England Temperature (CET) dataset (Parker et al., 1992) is used to characterise the daily variability of temperature over England. This dataset is chosen based on its long record which allows better characterisation of the extreme temperatures. The daily CET timeseries is used, from 1850 to 2017, all days of the year are included in the analysis. To estimate global-mean temperature changes over the same period, the HadCRUT4 dataset (version 4.6.0.0) is used (Morice et al., 2012). Since we do not examine the impact of decadal timescale climate variability on the health system, the decadally smoothed version of the HadCRUT4 dataset is used. Global mean temperatures in the HadCRUT4 dataset are expressed as anomalies from the 1961–1990 mean.

To remove the impact of climate change from this time series prior to some calculation we follow a simple method used by van Oldenborgh (2007). First the linear regression between the CET and global-mean HadCRUT4 timeseries is calculated. The regression equation for this fit (where all terms are in degree centigrade) is:

$$T_{\mathrm{CET}} = 9.61 + 1.28\, T_{\mathrm{HadCRUT4}}$$

Both of the terms in this fit are significant at the 0.05 level. A timeseries of the part of the T_{CET} which can be linearly related to the global-mean HadCRUT4 time series can then be calculated from this equation and is removed from the raw, daily CET time series.

$$T'_{\mathrm{CET}} = T_{\mathrm{CET}} - (9.61 + 1.28\, T_{\mathrm{HadCRUT4}})$$

Since the exposure-response relationships are defined for absolute temperature, for subsequent calculations it is necessary to add a constant offset to T'_{CET} to produce an adjusted CET time series with a fixed global mean temperature representative of a given period, T_{global}:

$$T_{\mathrm{CET_{adj}}} = T'_{\mathrm{CET}} + (9.61 + 1.28\, T_{global})$$

The resulting $T_{\mathrm{CET_{adj}}}$ time series is an estimate of the CET that would have occurred for each day in the record with an unvarying global mean climate. Three $T_{\mathrm{CET_{adj}}}$ time series are used in the study, one representative of pre-industrial climate ($T_{global} = -0.4$°C), one representative of the base, 1961–1990 climate ($T_{global} = 0$°C) and one representative of recent, 2000–2016 climate ($T_{global} = 0.5$°C).

2.1.2. Model simulations

Two large ensembles that have been previously used for climate attribution studies are used. Both ensembles provide large ensemble simulations of the recent climate with all historical climate forcings (Historical, including greenhouse gas forcing, aerosol and land-use changes) and with natural climate forcings only (Natural, including solar and volcanic forcings). As above, the daily mean temperature of each model run is used.

- Ensemble one. Fifty-member simulations of the Canadian Earth System Model version 2 (CanESM2) (Fyfe et al., 2017; Kirchmeier-Young et al., 2017). CanESM2 is described in detail in Arora et al. (2011). The model has relatively coarse horizontal resolution ($\approx 2.81°$) and has an equlibrium climate sensitivity (ECS) of 3.7 K (Mauritzen et al., 2017). The simulations run from 1950 to 2020, with standard, historical CMIP5 climate forcings used to 2005 and extended by forcings from the RCP8.5 scenario thereafter.
- Ensemble two. Fifteen-member, atmosphere only simulations of the Hadley Centre Global Environment Model version 3 (HadGEM3A-GA6) prepared as part of the EUCLEIA project (Met Office, 2016). The model is described in detail in Hewitt et al. (2011) and

Christidis et al. (2013). The version of HadGEM3A used has finer horizontal resolution (N216, $\approx 0.6^{\circ}$) than CanESM2 and has an ECS of 3.1 K (Senior et al., 2016). The simulations runs from 1959 to 2013 and have historical climate forcings up to the year 2005, followed by forcings from the RCP4.5 scenario to the end of the run.

Daily time series representing the two-metre temperature are extracted for a region corresponding to the CET for both model ensembles described in section 2. CET is defined as the average temperature of the region bounded by 2.5°W-0 longitude and 51–54°N, only points with a land fraction greater than 75% included in the average (King et al., 2015). Prior to analysis, quantile bias correction (Ho et al., 2012) is performed on each model ensemble, using the period 1961 to 1990 in the historical simulation as the base period for the calculation of the quantile mapping between observed and modelled CET.

2.1.3. Exposure-response relationships

To estimate the impact of cold weather on the health system the relationships published by Chalabi et al. (2016) are used. Two different metrics are calculated, the fraction of deaths attributable to cold weather and the fraction of hospital admissions due to the exacerbation of symptoms of COPD. In both cases, the fractional impact of temperatures on the health impacts can be calculated from the following equation:

$$i = \frac{(1+\theta_i)^{|T-\tau_i|} - 1}{(1+\theta_i)^{|T-\tau_i|}} \quad (1)$$

In this equation, i is the fractional health impact, θ_i is the increment in risk-ratio per degree below the threshold at which impacts from cold weather begin. τ_i is the threshold temperature at which health impacts begin. T is the daily-mean temperature. The resulting estimate i is the fraction of all cause mortality or COPD hospital admissions that can be attributed to cold weather for that particular day, assuming the same population vulnerability as in Hajat et al. (2016). There is little evidence that vulnerability to cold weather has changed since the mid-twentieth century (Arbuthnott et al., 2016) and so this assumption is reasonable. To estimate the absolute mortality or hospital admissions burden it would be necessary to multiply i by the observed daily mortality which is not available for this study. Parameters used in this model are taken from Chalabi et al. (2016) who in turn derived the parameters from the analysis of Hajat et al. (2016) which used time series regression analysis to derive the threshold and risk ratio parameters for observed mortality and morbidity data. Hajat et al. (2016) used mortality statistics for England for the period 1993 to 2006 and COPD admissions data for 1997 to 2011 to estimate the exposure response relationships. A key assumption of our work is that we use the long climate records and climate simulations to estimate how climate variability would affect a population with the same vulnerability to cold weather as derived from the Hajat et al. (2016) study. It is very likely that in the past, due to a wide range of societal and healthcare changes, that UK society had a different vulnerability to cold weather. This study does not seek to determine the impacts of changes in vulnerability to cold weather on the overall stress on the health system. Rather, we assume that the exposure-response relationships published by Chalabi et al. (2016) are a representative measure of vulnerability for the current UK population. There are some significant regional variations in the exposure-response relationships revealed by Hajat et al. (2016) and previous studies, but we choose not to focus on these regional data here since this would limit the amount of meteorological data which could be used to investigate the long-term climate changes which concern us here.

For each day in the CET observations or the estimate derived from the model simulations, Eq. (1) is used to estimate the fraction of mortality or hospital admissions that can be attributed to the observed temperature (hereafter attributable mortality and attributable admissions). Note that the attributable mortality or hospital admissions include the lagged effects of cold weather discussed by Gasparrini et al. (2015). Table 1 shows the parameters used for calculating attributable mortality and admissions.

Table 1
Parameter values used in the exposure-response model for mortality and COPD hospital admissions.

Parameter	Mortality	Admissions
θ_i	0.0384	0.084
τ_i	$5^{\circ}C$	$8^{\circ}C$

2.1.4. Weather regime classification

Weather regimes are identified using a standard diagnostic based on an empirical orthogonal function (EOF) analysis of 10-day low-pass filtered normalized 500 hPa geopotential height anomalies (Z500') and k-means clustering in the phase space spanned by the first seven EOFs (e.g. Michelangeli et al., 1995; Cassou, 2008; Ferranti et al., 2015). Geopotential height anomalies are defined with respect to the 90 day running mean of the climatology for the respective date. Data are taken six-hourly from the European Centre for Medium-range Weather Forecasts (ECMWF) Reanalyis Interim (ERA-Interim) spanning the period 1979–2016. The EOF analysis is performed in the Euro-Atlantic sector (80 W-40E, 30N–90N) and consistent with the diagnostic used in Grams et al. (2017) but limited to winter months (DJF/NDJFM). Note that in contrast to the bimodal NAO or AO, which are typically derived from the first EOF explaining about 20–25% of the variance, the WRs used here are based on the seven leading EOFs explaining about 85% of the variance and thus cover almost the full range of large-scale atmospheric flow variability. Where no clear weather regime is identified, days are classified as No Regime (NoReg).

2.1.5. Re-analysis data

To analyse the structure of atmospheric flows during winter pressure days, the ECWMF 20th Century (ERA-20C, Poli et al. (2016)) reanalysis dataset is used rather than the ERA-Interim dataset. The longer ERA-20C record makes it possible to analyse a large number of extreme events including those prior to the satellite era. The entire ERA-20C record is used, beginning on the 1st January 1900 and ending 31st December 2010. Several fields from the ERA-20C are used, including mean sea-level pressure, surface temperature, 1000 hPa and 500 hPa geopotential height. Daily means of all fields are calculated by averaging the 00, 06, 12 and 18Z output.

2.1.6. Software packages used

A number of open-source software packages are used for the analysis in this study. To fit extreme value distributions to the data, the extRemes 2.0 package for R (Gilleland and Katz, 2016) is used. In all cases, the function, fevd, is used to fit a Generalised Extreme Value (GEV) distribution to annual maximum daily mortality and admissions estimates. The model is fit using the default maximum likelihood estimation. Bootstrap confidence intervals are estimated for the calculations in Figs. 2 and 3 using the Bootstrapped package for python (Beecher et al., 2017). Standard options are used in all cases, all confidence estimates are made with 10,000 bootstrap with replacement samples.

3. Results

3.1. Impacts of climate change

Before quantifying the impact of different weather regimes on winter pressure days, it is important to first quantify how the long-term context of a warming climate has reduced their risk. In this analysis,

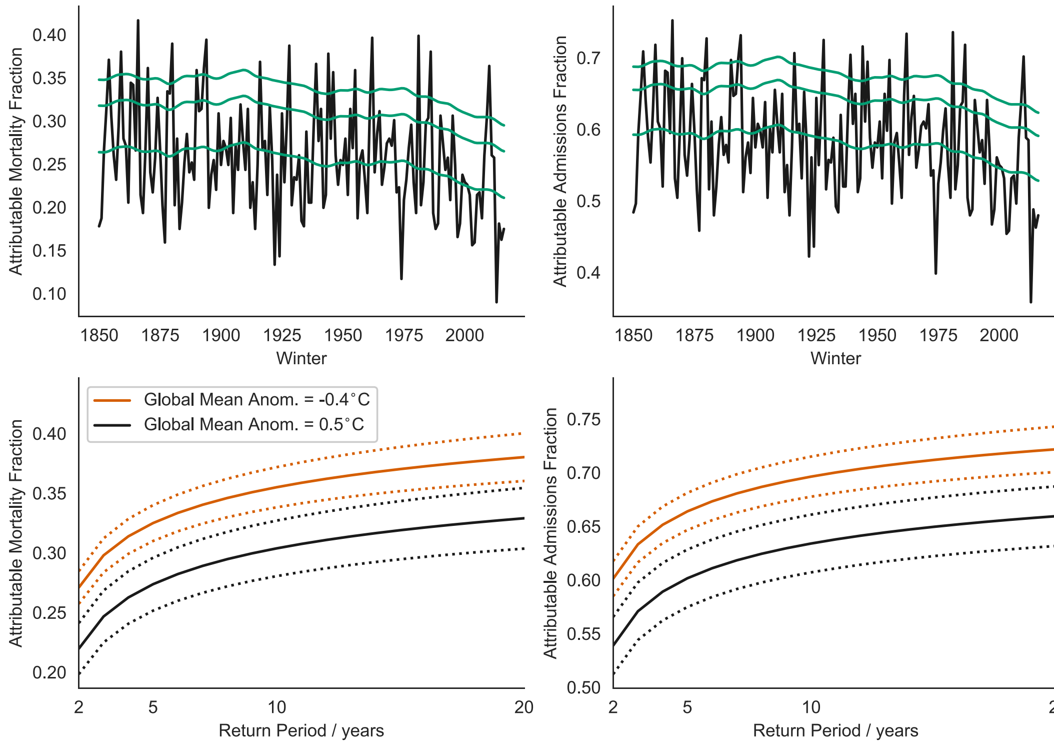

Fig. 1. Timeseries of annual attributable extreme mortality and admissions (black lines, top panel). Time-evolving two-year, five-year and ten-year return periods are also shown in green lines. Bottom panels show return periods for global mean temperature anomalies of −0.4 (red line, consistent with the pre-industrial baseline) and 0.5 (black line, consistent with the period 2000–2016). (For interpretation of the references to colour in this figure legend, the reader is referred to the Web version of this article).

changes in risk due to the ageing UK population are ignored since the aim is to isolate the meteorological drivers of cold weather stress on winter pressure days. As noted in, for example, Hajat et al. (2016) an increase in the population of adults age 75 and older has likely increased the vulnerability of the health system to extreme weather due to the enhanced vulnerability of this age group to cold weather.

Estimates of the annual maximum of fractional daily mortality and hospital admissions derived from the unadjusted, T_{CET} time series since 1850 are shown in the top two panels of Fig. 1. In addition to the large year-to-year variability, there has been a clear decline of the annual maxima since 1975. Following van Oldenborgh (2007), one method of understanding the extent to which this decline has been influenced by climate change is to fit a generalised extreme value (GEV) distribution to the data with additional predictors that characterise changes to the parameters of the distribution (location, scale and shape) related to changes in the global mean temperature (derived from T_{HadCRUT4}).

To determine where there have been robust changes to the parameters of the GEV distribution for annual maximum attributable mortality and admissions a series of experiments were performed comparing a null fit of the GEV in which all the parameters are assumed to be stationary to alternative fits in which the location, scale and shape parameters are assumed to be proportional to the global mean temperature. A likelihood ratio test is used to compare the goodness of fit of each alternative, non-stationary model with the null, stationary model. Neither the model with the shape parameter dependent on the global mean temperature nor the model with the scale parameter dependent on the global mean has a significantly better fit to the data than the stationary model. In contrast, as expected, the model in which the location parameter depends on the global mean temperature does have a significantly better fit to the data than the stationary model ($p < 0.0005$). The best fit parameters of this statistical fit for annual mean attributable mortality and admissions are shown in Table 2.

Results from the non-stationary model with variable location are shown in Fig. 1 in two ways. In the top two panels, the return levels of extremes with 2, 5 and 10-year return periods are shown in the green lines. The downward trend in the severity of extremes (consistent with global mean climate trends) is clearly shown, particularly over the most recent thirty years, which gives additional confidence in the fit of the model. In the bottom panels, return periods derived from the GEV model with global mean temperature anomalies of $-0.4^{\circ}C$ (pre-industrial values, red line) and $0.5^{\circ}C$ (consistent with the average temperature during the period 2000–2016, black line) are shown. For the moderate extremes of mortality and admissions shown in the bottom panel of Fig. 1, with return periods less than 20 years, the modern climate represents a clear reduction in risk compared to the pre-industrial climate.

It is useful for this and subsequent analysis to define a threshold level of mortality and admissions that would indicate a winter pressure day. We choose the five-year return level as a representative moderate extreme. Based on the two GEV models, the five-year return level for a global mean temperature anomaly of 0°C (i.e. the 1960–1990 baseline) is 30% of deaths and 64% of admissions. In the pre-industrial climate (global-mean temperature anomaly $= -0.4^{\circ}C$) the mean return period of an annual, daily maximum of 30% of attributable deaths is 3.3 years ($p(M > 0.3) = 0.31$), while for the modern climate (global-mean temperature anomaly $= 0.5\,^{\circ}C$) it is 9.6 years ($p(M > 0.3) = 0.1$). This change in probability is equivalent to a Fraction of Attributable Risk (FAR) of -1.94 when comparing the 2000–2016 climate to the pre-industrial climate and -0.92 when comparing the 2000–2016 climate to the 1960–1990 climate. We return to the FAR in the following section. It is clear therefore, that the risks of health system stress events are smaller under the current climate than at other times in the recent past.

3.2. Anthropogenic influence

To quantify the extent to which these changes in risk can be attributed to anthropogenic influences, model experiments that separate the effects of natural and human climate forcings are required. The

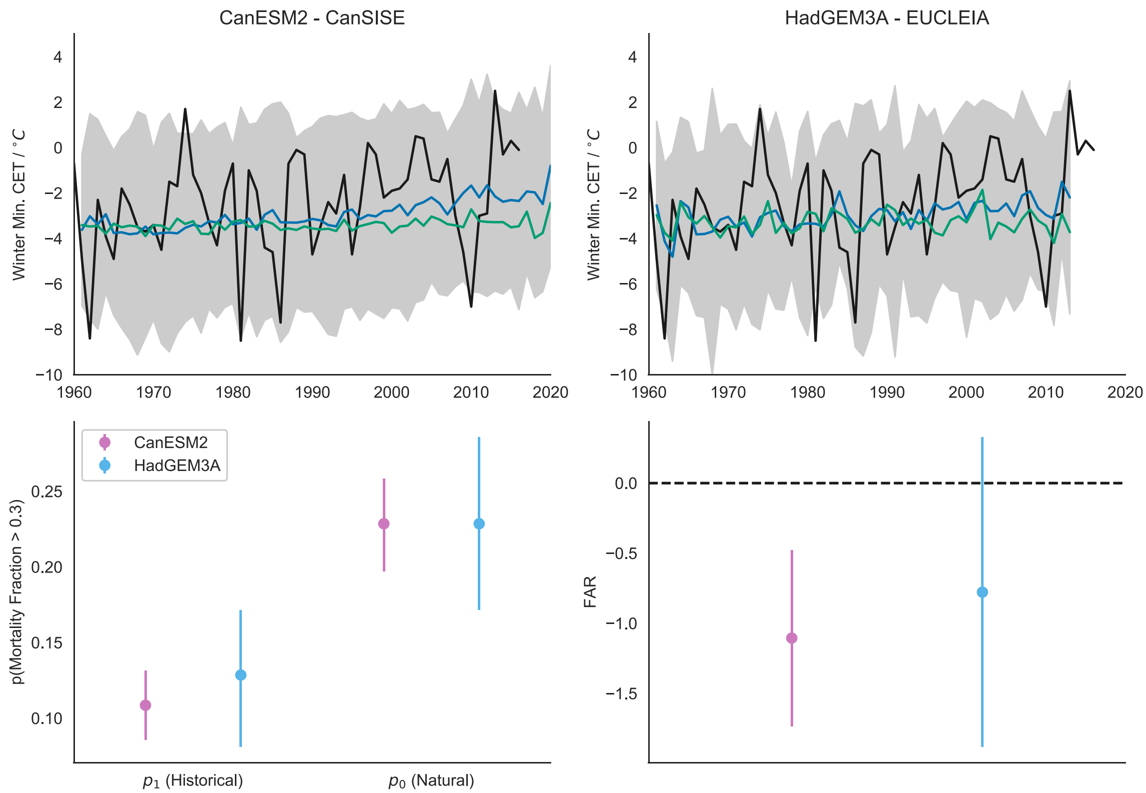

Fig. 2. Attribution of changes in the risk of large mortality events to anthropogenic climate forcings. Top panels show timeseries of annual winter temperature minimum from CET timeseries (black line) and as simulated by the CanESM2 (left column) and HadGEM3A (right column) models. Grey shading shows the 99% confidence range of annual CET minima estimated from standard deviation of the ensemble with historical climate forcings and 50 members for CanESM2 and 15 members for HadGEM3A. The ensemble average for the ensemble with historical climate forcings is shown in the blue line and with natural climate forcings only is shown in the green line. The bottom left panel shows the probability of the daily annual maximum attributable fractional mortality exceeding 30% of deaths for the historical simulations (p_1) and for the natural simulations (p_0) in dots with a 95% confidence interval for each estimate shown as an error bar. Results for the CanESM2 ensemble are shown as magenta dots and lines and for the HadGEM3A as cyan dots and lines. The Fraction of Attibutable Risk (FAR, 1-(p_0/p_1)) for a daily annual maximum event exceeding 477 deaths is shown in the bottom right panel. (For interpretation of the references to colour in this figure legend, the reader is referred to the Web version of this article).

widely used methodology of Pall et al. (2011) is used to determine the difference in probability of extreme mortality events in model simulations of the historical climate (p_1) and in a counter-factual ensemble in which only natural climate forcings are present (p_0).

For both the models used, there is a good match with the annual minimum daily-mean CET values (Fig. 2). The grey shading, which represents the distribution of annual minimum daily-mean temperature in the two models, matches well with the observed CET (black line), indicating that the quantile matching has been successful. The blue and green lines, which represent the average daily maximum shown in the model ensemble with historical forcings and with natural forcings, are clearly separated after the mid-1990s in both simulations.

To assess the change in mortality risk that can be attributed to anthropogenic climate forcings, the daily time series of bias corrected CET is used to generate an ensemble of estimates for daily attributable mortality. The probability of observing a annual, daily maximum of mortality greater than 0.3 during the period 2000 to 2013 is estimated from each model ensemble. The uncertainty in this quantity is estimated from a 10,000 member bootstrap sample with replacement. The probability of a mortality extreme for the historical simulations (p_1) is shown in the bottom left panel of Fig. 2 and is close to 0.1 for both ensemble. In the counter-factual, natural forcing only simulations (p_0) the probability of observing the same annual extreme mortality is approximately doubled. These probability estimates can be used to estimate the FAR for each model which is shown in the bottom right panel of Fig. 2. For CanESM2, the mean estimate of the FAR is −1.1 and for HadGEM3A, the mean estimate is −0.78. Uncertainty estimates for the HadGEM3A ensemble overlap zero.

From these two pieces of analysis, we conclude that, in these two climate models, the risk of winter pressure days has been approximately halved by anthropogenic forcing of the climate system. Therefore in planning for the long term impacts of cold weather on the health system, the impacts of anthropogenic climate change must be considered since they can already be clearly detected and attributed.

However, it is also clear that there is substantial year to year variability in attributable mortality and extreme minimum temperature (see for example the annual noise present in the black lines representing annual maximum mortality in Fig. 1).

3.3. *Weather regimes*

To consider the impacts of weather variability on the health system, we now compare winter pressure days present during different large-scale WR. Using the WR dataset described in the methods section, we identify all lifecycles of each WR present during the analysis period (NDJFM, 1979–2016) and filter out periods with no clear regime signature (NoReg). In total, there are 76 ZO lifecycles, 57 GL lifecycles, 94 BL lifecycles and 74 AR lifecycles.

For each WR lifecycle and NoReg days, the average and extreme attributable mortality and hospital admissions fraction are calculated. Fig. 3 shows the mean average mortality and hospital admissions fraction for WR of each type (right panel) and the proportion of the lifecycles with peak fractional mortality or hospital admissions that exceed the five-year return period for the annual daily maximum. For

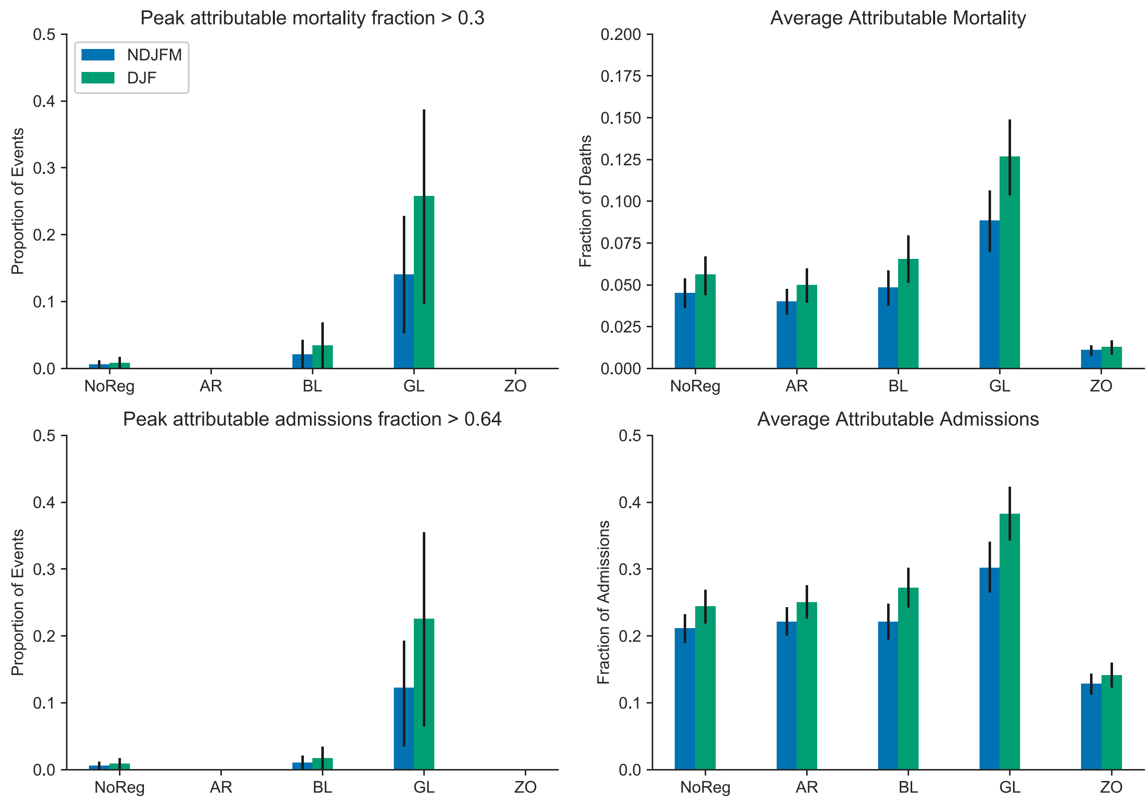

Fig. 3. Diagnostics of fraction of attributable mortality and admissions during four different weather regimes. Left column shows proportion of weather regime events that have peak attributable mortality above 0.3 deaths (top left) or 0.64 hospital admissions (bottom left). Blue bars show events during the extended winter NDJFM, green bars show events during mid-winter (DJF). The right column shows the average attributable mortality or admissions for a day in each weather regime for the same periods. Weather regimes are Atlantic Ridge (AR), Scandinavian Blocking (BL), Greenland Blocking (GL) and Zonal (ZO). Where there is no clear weather regime (NoReg), theses days are filtered out and considered separately. 95% confidence intervals for each estimate are shown as black error bars. (For interpretation of the references to colour in this figure legend, the reader is referred to the Web version of this article).

Table 2
Best fit GEV parameters for Non-Stationary model with variable location. T indicates global mean temperature. Standard errors for each parameter are shown in brackets.

Parameter	Mortality	Admissions
Scale	0.057 (0.0034)	0.07 (0.0042)
Shape	−0.18 (0.050)	−0.26 (0.052)
Location	0.22 (0.005) - 0.057 (0.016) T	0.55 (0.006) - 0.069 (0.019) T

this calculation, attributable mortality fraction estimates with the baseline $T_{\mathrm{CET}_{\mathrm{adj}}}$ (i.e. global mean temperature anomaly of zero) are used to avoid including the climate change signal described in the previous section in the calculation.

As can be seen from the right panels of Fig. 3, there is a clear difference in the average attributable mortality and admissions fraction for the GL regime compared to the other three regimes. On average, during a GL regime in DJF, more than 12.7% of deaths and 38% of hospital admissions can be attributed to cold weather. In contrast in the BL regime (the regime with the next largest burden), only 6.5% of deaths and 27% of hospital admissions can be attributed to cold weather. The other two regimes have a lower burden.

Of equal importance to the change of average mortality and admissions, is the change in likelihood of extreme events associated with each regime. The left panels of Fig. 3 show the proportion of regime lifecycles in which the peak attributable mortality crosses the five-year return threshold used in previous analysis. This only occurs with significant frequency for the GL regime. Eight of the thirty-one GL lifecycles (or 25%) have peak attributable mortality above the 0.3 threshold. In comparison, only two other regime lifecycles (BL during January 1982 and February 1991) have peak attributable mortality above this level.

Although this analysis shows that stresses to the health system are most acute during the GL weather regime, it is important to be clear that this risk can result from a relatively broad range of synoptic conditions. To illustrate this, Figs. 4 and 5 show daily mean synoptic maps of mean sea-level pressure and surface temperature fields and anomalies for the five most recent cases in which attributable mortality fraction exceeded the five-year return period threshold. The top left panel in each figure shows the average field and anomaly for all cases since 1900 (Table 3) shows a list of these cases along with their attributable mortality fraction and CET anomalies). Although four of the five cases occur during the GL regime, their synoptic structure can be dominated by high pressure to the North-West of the UK (as on 28th November 2010), by high pressure to the North-East of the UK (as on 7th February 1991 and 12th January 1987) or relatively weak pressure gradients (as on 7th January 2010 and 28th December 1995). The common feature uniting all the cases, and weakly visible in the average of all cases is that the surface flow over the UK is predominantly easterly and is associated with advection of very cold air masses from the European continent. In all cases, Fig. 5 shows daily mean surface temperatures below freezing (thick contour) over a large part of North-Western Europe and Scandinavia in addition to the UK. This pattern of extreme cold conditions is consistent with many other studies including for example de Vries et al. (2012).

4. Conclusions

Motivated by recent winters in which the UK health system has been under severe pressure, this study sets out to examine the weather and

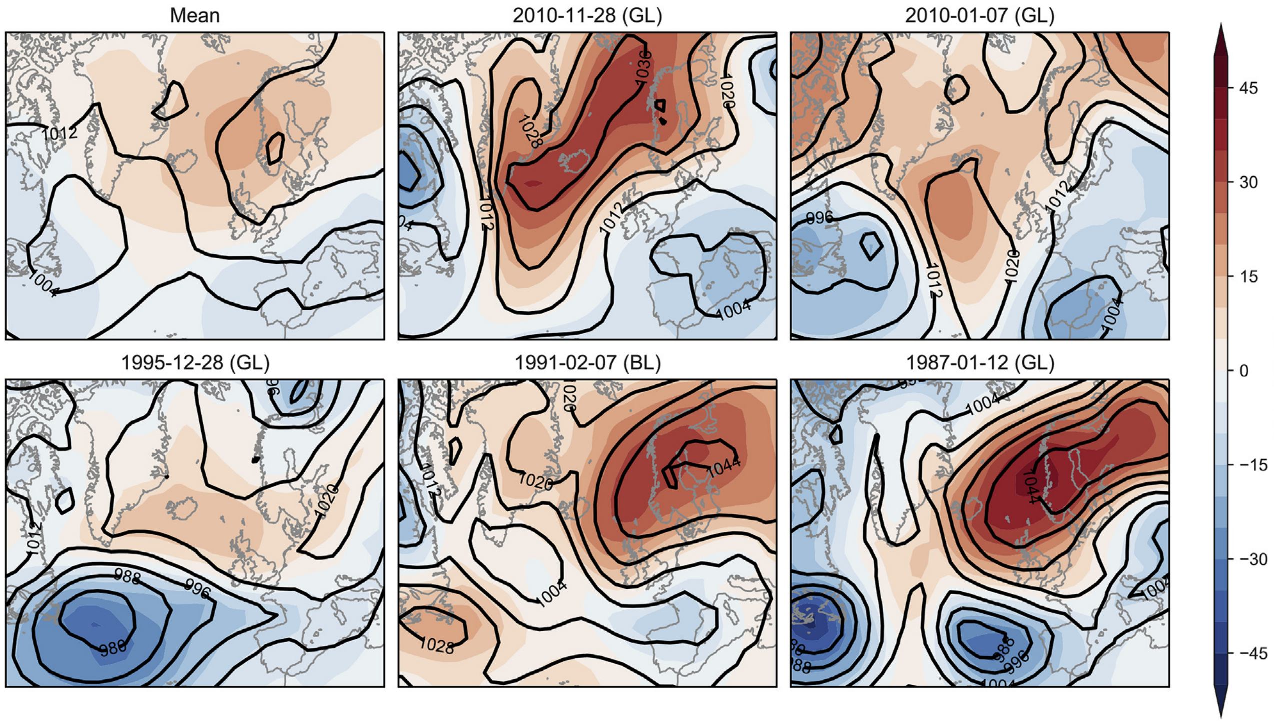

Fig. 4. Daily average, mean sea-level pressure on the day of occurrence of days when the attributable fraction of mortality exceeds the five-year return period. All data are from the ERA-20C re-analysis. In each panel, absolute mean sea-level pressure in hPa is shown in the contours with a contour interval of 8 hPa. Anomalies from the daily climatology for the years 1961–1990 is shown in the coloured shading. The top left panel shows the average mean sea-level pressure and mean sea-level pressure anomaly for all cases in Table 3.

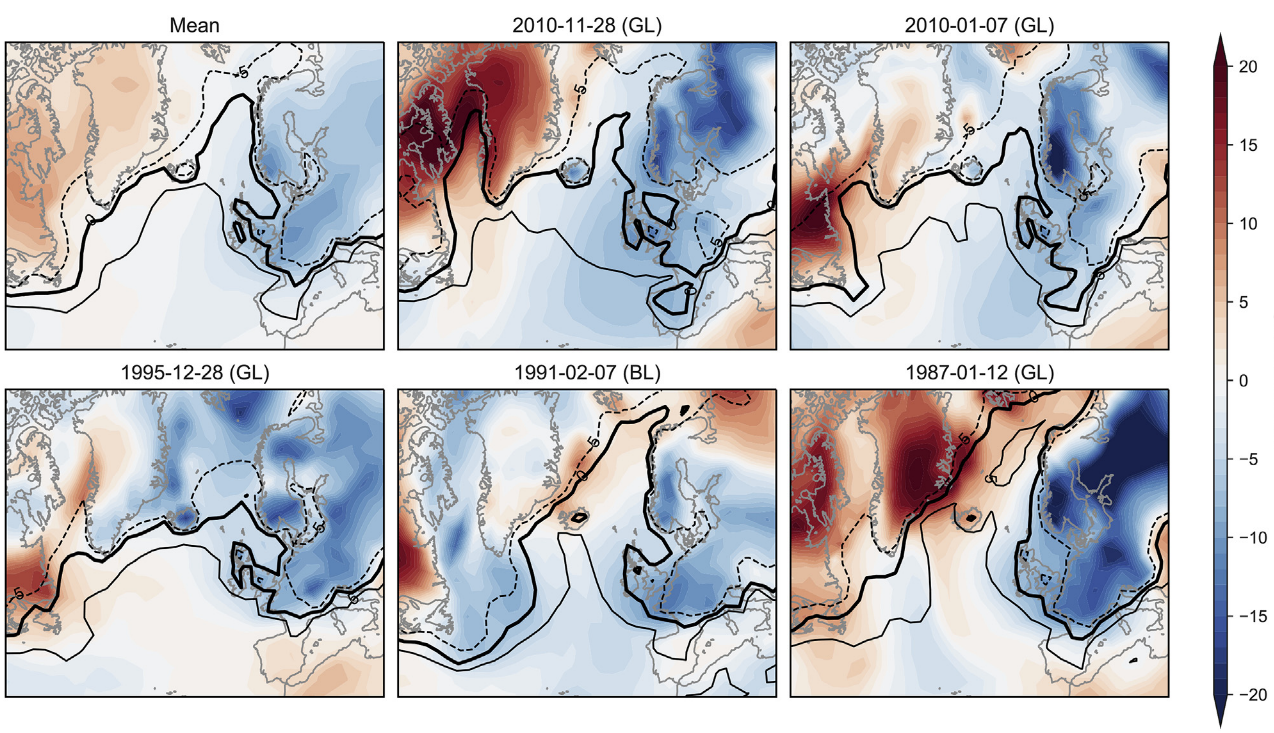

Fig. 5. Daily average, 2-m temperature on the day of occurrence of days when the attributable fraction of mortality exceeds the five-year return period. All data are from the ERA-20C re-analysis. In each panel, the absolute 2-m temperature is shown in the contours. The thick solid contour shows 0 $^{\circ}C$, the thin solid contour shows 5 $^{\circ}C$ and the dashed contour shows $-5\,^{\circ}C$. Anomalies from the daily climatology for the years 1961–1990 are shown in the coloured shading. The top left panel shows the average mean sea-level pressure and mean sea-level pressure anomaly for all cases in Table 3.

Table 3
Extreme mortality events. Mortality and Admissions are show as attributable daily fraction.

Date	CET	CET_{adj}	Attributable Mortality	Attributable $Mortality_{adj}$	Attributable Admissions	Attributable $Admissions_{adj}$
1917-02-07	−7.2	−6.8	36	35	70	69
1929-02-15	−8.0	−7.7	38	38	72	71
1940-01-21	−7.1	−7.1	36	36	70	70
1942-01-21	−5.0	−5.0	31	31	64	64
1945-01-26	−7.6	−7.6	37	37	71	71
1947-01-29	−6.4	−6.4	34	34	68	68
1954-02-02	−5.0	−4.9	31	31	64	64
1956-02-01	−6.8	−6.7	35	35	69	69
1962-01-01	−4.9	−4.9	31	31	64	64
1963-01-23	−8.4	−8.3	39	39	73	73
1966-01-19	−4.9	−4.8	31	30	64	64
1981-12-12	−8.5	−8.6	39	40	73	73
1985-01-17	−4.4	−4.5	29	30	63	63
1986-02-10	−4.6	−4.7	30	30	63	64
1987-01-12	−7.7	−7.8	38	38	71	72
1991-02-07	−4.7	−4.9	30	31	64	64
1995-12-28	−4.7	−5.1	30	31	64	65
2010-01-07	−4.6	−5.2	30	31	63	65
2010-11-28	−4.0	−4.6	28	30	62	63

climate drivers that may have contributed to these winter pressures. Two potential drivers of changes to cold-weather related stresses on the system were considered, climate change and the large-scale weather regime.

Based both on the analysis of the long CET temperature record and on model simulations from two climate models, a reduction of the risk of winter extreme mortality and admissions and assumed winter pressures can be detected and attributed to anthropogenic climate forcings. For the period since the year 2000 and a fixed vulnerability of the population to cold temperatures, a representative fractional daily mortality extreme (30% of deaths) would have been 1.5 times more likely without anthropogenic forcings.

In addition to the relatively slow change in risk associated with climate change, year to year variability in winter pressure days is substantial. Extremes of mortality and admissions occur during weeks in which the large-scale atmospheric flow is in the Greenland Blocking regime and surface advection of cold air masses from the European mainland can occur.

In order to prepare for and mitigate the impact of cold weather extremes on the UK health system, skilful and reliable weather forecasts of cold conditions are required. Extending the range over which adverse cold weather health impacts are currently anticipated, which is typically only with a lead time of one week for the UK, could aid in preparing for them. Efforts to improve forecasting on the sub-seasonal time range are currently the focus of significant amounts of international activity (e.g. Vitart et al., 2017). Our study shows that one aspect of understanding and improving medium-range and sub-seasonal forecast skill for health applications might be a focus on the predictability of the GL weather regime (e.g. Ferranti et al., 2015), due to its prominent role in driving health system impacts. Recent work by Ferranti et al. (2018) shows that predicting regimes leading to cold conditions on sub-seasonal timescales is beginning to be possible.

This study makes several key assumptions about the impact of cold weather on the health system. Most notably, we assume that the exposure-response relationships derived by Hajat et al. (2016) are relevant to determining the sensitivity of mortality and admissions in the current population to weather variability. While this is a significant assumption, it seems unlikely that these relationships are significantly different in the current population and this is supported by meta-analysis of the literature (e.g. Arbuthnott et al., 2016). Our assumption that daily extremes in attributable mortality and admissions can be used as a proxy for pressures on the health system is also important in the analysis. However, since no other clear relationships between temperature and more refined diagnostics of impacts on the health system have been developed for them UK, these relationships are likely a good first proxy for health system impacts. No account is made for the impact of weather conditions on the spread and severity of communicable diseases (for example Influenza) which make a significant contribution to health service pressures during winter. A future study could make use of recent work developing forecasting system for influenza in the USA to model these winter impacts (Shaman et al., 2013). Similarly, changes in many other social and economic factors have and will continue to contribute ill-health during winter including housing quality and availability, energy prices and the impacts of air pollution. Our analysis of the role of anthropogenic forcings in the reduction of risk of days with substantial mortality relies on the fidelity of the two modelling systems that are used and the climate forcings used in the experiments analysed. The wide use of these two sets of experiments in other studies should increase confidence that the quantification of changes in risk are robust and meaningful.

Acknowledgments

We thank two anonymous reviewers for their insightful comments which really helped to improve the manuscript. The contribution of CMG was supported by the Helmholtz Association under Young Investigator Grant VH-NG-1243. AJCP completed this work while on sabbatical at the European Centre for Medium-Range Weather Forecasts and University College London. RWL and AJCP are supported by the Belmont Forum project InterDec (NE/P006787/1). RWA is supported by a Wellcome Trust Clinical Research Career Development Fellowship (206602/Z/17/Z).

Appendix A. Supplementary data

Supplementary data to this article can be found online at https://doi.org/10.1016/j.wace.2019.100218.

References

Analitis, A., Katsouyanni, K., Biggeri, A., Baccini, M., Forsberg, B., Bisanti, L., Kirchmayer, U., Ballester, F., Cadum, E., Goodman, P., et al., 2008. Effects of cold weather on mortality: results from 15 european cities within the PHEWE project. Am. J. Epidemiol. 168 (12), 1397–1408.

Arbuthnott, K., Hajat, S., Heaviside, C., Vardoulakis, S., 2016. Changes in population susceptibility to heat and cold over time: assessing adaptation to climate change. Environ. Health 15 (1), S33.

Arora, V., Scinocca, J., Boer, G., Christian, J., Denman, K., Flato, G., Kharin, V., Lee, W., Merryfield, W., 2011. Carbon emission limits required to satisfy future representative concentration pathways of greenhouse gases. Geophys. Res. Lett. 38 (5).
Beecher, S., van der Drift, D., Martin, D., Vaas, L., Goder, S., Lim, B., Langner, 2017. Bootstrapped - confidence intervals made easy. https://github.com/facebookincubator/bootstrapped.
Cassou, C., 2008. Intraseasonal interaction between the Madden–Julian oscillation and the North Atlantic Oscillation. Nature 455 (7212), 523.
Chalabi, Z., Hajat, S., Wilkinson, P., Erens, B., Jones, L., Mays, N., 2016. Evaluation of the cold weather plan for england: modelling of cost-effectiveness. Public Health 137, 13–19.
Christidis, N., Stott, P.A., Scaife, A.A., Arribas, A., Jones, G.S., Copsey, D., Knight, J.R., Tennant, W.J., 2013. A new hadgem3-a-based system for attribution of weather-and climate-related extreme events. J. Clim. 26 (9), 2756–2783.
de Vries, H., Haarsma, R.J., Hazeleger, W., 2012. Western european cold spells in current and future climate. Geophys. Res. Lett. 39 (4).
Elliot, A.J., Cross, K.W., Fleming, D.M., 2008. Acute respiratory infections and winter pressures on hospital admissions in england and wales 1990–2005. J. Public Health 30 (1), 91–98.
Ferranti, L., Corti, S., Janousek, M., 2015. Flow-dependent verification of the ECMWF ensemble over the euro-atlantic sector. Q. J. R. Meteorol. Soc. 141 (688), 916–924.
Ferranti, L., Magnusson, L., Vitart, F., Richardson, D., 2018. How far in advance can we predict changes in large-scale flow leading to severe cold conditions in europe? Q. J. R. Meteorol. Soc. 144, 1788–1802.
Fyfe, J.C., Derksen, C., Mudryk, L., Flato, G.M., Santer, B.D., Swart, N.C., Molotch, N.P., Zhang, X., Wan, H., Arora, V.K., et al., 2017. Large near-term projected snowpack loss over the western United States. Nat. Commun. 8, 14996.
Gardner, T., 2018. NHS Winter Pressures: Going Home from Hospital. https://www.health.org.uk/blog/nhs-winter-pressures-going-home-hospital.
Gasparrini, A., Guo, Y., Hashizume, M., Lavigne, E., Zanobetti, A., Schwartz, J., Tobias, A., Tong, S., Rocklöv, J., Forsberg, B., et al., 2015. Mortality risk attributable to high and low ambient temperature: a multicountry observational study. The Lancet 386 (9991), 369–375.
Gilleland, E., Katz, R.W., et al., 2016. extRemes 2.0: an extreme value analysis package in R. J. Stat. Softw. 72 (8), 1–39.
Grams, C.M., Beerli, R., Pfenninger, S., Staffell, I., Wernli, H., 2017. Balancing europe's wind-power output through spatial deployment informed by weather regimes. Nat. Clim. Chang. 7 (8), 557.
Hajat, S., 2017. Health effects of milder winters: a review of evidence from the United Kingdom. Environ. Health 16 (1), 109.
Hajat, S., Chalabi, Z., Wilkinson, P., Erens, B., Jones, L., Mays, N., 2016. Public health vulnerability to wintertime weather: time-series regression and episode analyses of national mortality and morbidity databases to inform the cold weather plan for england. Public Health 137, 26–34.
Hajat, S., Kovats, R.S., Lachowycz, K., 2007. Heat-related and cold-related deaths in England and Wales: who is at risk? Occup. Environ. Med. 64 (2), 93–100.
Hajat, S., Vardoulakis, S., Heaviside, C., Eggen, B., 2014. Climate change effects on human health: projections of temperature-related mortality for the UK during the 2020s, 2050s and 2080s. J. Epidemiol. Community Health 68 (7), 641–648.
Hall, R.J., Hanna, E., 2018. North atlantic circulation indices: links with summer and winter UK temperature and precipitation and implications for seasonal forecasting. Int. J. Climatol. 38, e660–e677.
Hawkes, N., 2018. NHS data show a&e patients waiting longer and big rise in gp flu consultations. BMJ Br. Med. J. (Clin. Res. Ed.) 360.
Hewitt, H., Copsey, D., Culverwell, I., Harris, C., Hill, R., Keen, A., McLaren, A., Hunke, E., 2011. Design and implementation of the infrastructure of hadgem3: the next-generation met office climate modelling system. Geosci. Model Dev. (GMD) 4 (2), 223–253.
Ho, C.K., Stephenson, D.B., Collins, M., Ferro, C.A., Brown, S.J., 2012. Calibration strategies: a source of additional uncertainty in climate change projections. Bull. Am. Meteorol. Soc. 93 (1), 21–26.
Hull, S.A., Homer, K., Boomla, K., Robson, J., Ashworth, M., 2018. Population and patient factors affecting emergency department attendance in london: retrospective cohort analysis of linked primary and secondary care records. Br. J. Gen. Pract. 68 (668), e157–e167. https://doi.org/10.3399/bjgp18X694397.
Iacobucci, G., 2017. A service under pressure. BMJ Br. Med. J. (Clin. Res. Ed.) 356.
Iacobucci, G., 2018. NHS Cancels Planned Surgery and Outpatient Appointments in Response to Winter Crisis.
King, A.D., van Oldenborgh, G.J., Karoly, D.J., Lewis, S.C., Cullen, H., 2015. Attribution of the record high Central England temperature of 2014 to anthropogenic influences. Environ. Res. Lett. 10 (5), 054002.
Kirchmeier-Young, M.C., Zwiers, F.W., Gillett, N.P., Cannon, A.J., 2017. Attributing extreme fire risk in western Canada to human emissions. Clim. Change 144 (2), 365–379.
Liddell, C., Morris, C., Thomson, H., Guiney, C., 2016. Excess winter deaths in 30 european countries 1980–2013: a critical review of methods. J. Public Health 38 (4), 806–814.
Mauritzen, C., Zivkovic, T., Veldore, V., 2017. On the relationship between climate sensitivity and modelling uncertainty. Tellus A Dyn. Meteorol. Oceanogr. 69 (1), 1327765.
Met Office, 2016. Eucleia Multi-Decadal Historical Natural-Only Forcings (1960-2013), a Numerical Simulation Data Produced by the uk Met Office Using Hadgem3-A. http://catalogue.ceda.ac.uk/uuid/b1e2f38d1df048808625437764ca9578.
Michelangeli, P.-A., Vautard, R., Legras, B., 1995. Weather regimes: recurrence and quasi stationarity. J. Atmos. Sci. 52 (8), 1237–1256.
Mitchell, D., Heaviside, C., Vardoulakis, S., Huntingford, C., Masato, G., Guillod, B.P., Frumhoff, P., Bowery, A., Wallom, D., Allen, M., 2016. Attributing human mortality during extreme heat waves to anthropogenic climate change. Environ. Res. Lett. 11 (7), 074006.
Morice, C.P., Kennedy, J.J., Rayner, N.A., Jones, P.D., 2012. Quantifying uncertainties in global and regional temperature change using an ensemble of observational estimates: the HadCRUT4 data set. J. Geophys. Res.: Atmosphere 117 (D8).
Neal, R., Fereday, D., Crocker, R., Comer, R.E., 2016. A flexible approach to defining weather patterns and their application in weather forecasting over europe. Meteorol. Appl. 23 (3), 389–400.
Pall, P., Aina, T., Stone, D.A., Stott, P.A., Nozawa, T., Hilberts, A.G., Lohmann, D., Allen, M.R., 2011. Anthropogenic greenhouse gas contribution to flood risk in England and Wales in autumn 2000. Nature 470 (7334), 382.
Parker, D.E., Legg, T.P., Folland, C.K., 1992. A new daily central England temperature series, 1772–1991. Int. J. Climatol. 12 (4), 317–342.
Peterson, T.C., Stott, P.A., Herring, S., 2012. Explaining extreme events of 2011 from a climate perspective. Bull. Am. Meteorol. Soc. 93 (7), 1041–1067.
Poli, P., Hersbach, H., Dee, D.P., Berrisford, P., Simmons, A.J., Vitart, F., Laloyaux, P., Tan, D.G., Peubey, C., Thépaut, J.-N., et al., 2016. ERA-20C: an atmospheric reanalysis of the twentieth century. J. Clim. 29 (11), 4083–4097.
Public Health England, 2017. The Cold Weather Plan for England. https://assets.publishing.service.gov.uk/government/uploads/system/uploads/attachment_data/file/652564/Cold_Weather_Plan_2017.pdf.
Senior, C.A., Andrews, T., Burton, C., Chadwick, R., Copsey, D., Graham, T., Hyder, P., Jackson, L., McDonald, R., Ridley, J., et al., 2016. Idealized climate change simulations with a high-resolution physical model: HadGEM3-GC2. J. Adv. Model. Earth Syst. 8 (2), 813–830.
Shaman, J., Karspeck, A., Yang, W., Tamerius, J., Lipsitch, M., 2013. Real-time influenza forecasts during the 2012–2013 season. Nat. Commun. 4, 2837.
Stone, D.A., Allen, M.R., 2005. The end-to-end attribution problem: from emissions to impacts. Clim. Change 71 (3), 303–318.
van Oldenborgh, G., 2007. How unusual was autumn 2006 in europe? Clim. Past 3 (4), 659–668.
Vautard, R., 1990. Multiple weather regimes over the north atlantic: analysis of precursors and successors. Mon. Weather Rev. 118 (10), 2056–2081.
Vitart, F., Ardilouze, C., Bonet, A., Brookshaw, A., Chen, M., Codorean, C., Déqué, M., Ferranti, L., Fucile, E., Fuentes, M., et al., 2017. The subseasonal to seasonal (s2s) prediction project database. Bull. Am. Meteorol. Soc. 98 (1), 163–173.
Yiou, P., Nogaj, M., 2004. Extreme climatic events and weather regimes over the North Atlantic: when and where? Geophys. Res. Lett. 31 (7).